

# Prospects for macroscopic dark matter detection at space-based and suborbital experiments

Luis A. Anchordoqui,<sup>1,2,3</sup> Mario E. Bertaina,<sup>4</sup> Marco Casolino,<sup>5</sup> Johannes Eser,<sup>6</sup> John F. Krizmanic,<sup>7,8</sup> Angela V. Olinto,<sup>6</sup> A. Nepomuk Otte,<sup>9</sup> Thomas C. Paul,<sup>1</sup> Lech W. Piotrowski,<sup>10</sup> Mary Hall Reno,<sup>11</sup> Fred Sarazin,<sup>12</sup> Kenji Shinozaki,<sup>13</sup> Jorge F. Soriano,<sup>1,2</sup> Tonia M. Venters,<sup>7</sup> and Lawrence Wiencke<sup>12</sup>

<sup>1</sup>*Department of Physics and Astronomy, Lehman College, City University of New York, NY 10468, USA*

<sup>2</sup>*Department of Physics, Graduate Center, City University of New York, NY 10016, USA*

<sup>3</sup>*Department of Astrophysics, American Museum of Natural History, NY 10024, USA*

<sup>4</sup>*Dipartimento di Fisica, Università di Torino, Torino 10125, Italy*

<sup>5</sup>*Istituto Nazionale di Fisica Nucleare, Section of Roma Tor Vergata, Italy*

<sup>6</sup>*Department of Astronomy & Astrophysics, KICP, EFI, University of Chicago, Chicago, IL 60637, USA*

<sup>7</sup>*Astrophysics Science Division, NASA Goddard Space Flight Center, Greenbelt, MD 20771, USA*

<sup>8</sup>*University of Maryland, Baltimore County, Baltimore, MD 21250, USA*

<sup>9</sup>*Georgia Institute of Technology 837 State Street NW, Atlanta, Georgia 30332-0430, USA*

<sup>10</sup>*Faculty of Physics, University of Warsaw, Warsaw, Poland*

<sup>11</sup>*Department of Physics and Astronomy, University of Iowa, Iowa City, IA 52242, USA*

<sup>12</sup>*Department of Physics, Colorado School of Mines, Golden, CO 80401, USA*

<sup>13</sup>*National Centre for Nuclear Research, Lodz, 90-559, Poland*

(Dated: April 2021)

We compare two different formalisms for modeling the energy deposition of macroscopically sized/massive quark nuggets (a.k.a. macros) in the Earth's atmosphere. We show that for a reference mass of 1 g, there is a discrepancy in the macro luminosity of about 14 orders of magnitude between the predictions of the two formalisms. Armed with our finding we estimate the sensitivity for macro detection at space-based (Mini-EUSO and POEMMA) and suborbital (EUSO-SPB2) experiments.

The conventional textbook dark matter (DM) particle species is assumed to interact with Standard Model (SM) fields only gravitationally [1]. Actually, the cross section of the canonical weakly-interacting massive particle (WIMP) [2] to scatter from baryons is non-zero though small enough to be considered effectively zero for mass scales above a solar mass [3]. Yet, since the WIMP parameter space keeps shrinking due to null results at the LHC [4–6] and unsatisfactory answers from the WIMP search program using direct and indirect detection methods [7, 8], the case for alternative (and especially SM) candidates featuring stronger DM-baryon interactions has grown stronger, and attracted increasing attention.

Macroscopic DM is a general class of models with DM in a compact and composite state with a large radius and mass. Nuclearites and its dark quark nuggets cousins provide two compelling examples. Nuclearites are macroscopically sized nuggets of strange quark matter which could have been produced during the QCD phase transition in the early universe [9–12]. If this were the case then DM would have nuclear density,  $\rho_s \sim 3.6 \times 10^{14} \text{ g/cm}^3$  [13]. However, this constraint may be relaxed for the case of dark nuclearites as the dark quark nugget's energy density may span several orders of magnitude depending on the confinement scale and the magnitude of the dark baryon asymmetry [14]. Herein we refer to all such macroscopic DM candidates generically as macros [15], and following [16], we let the macro's energy density to vary in a generous range  $10^6 < \rho_m/(\text{g/cm}^3) < 10^{15}$ .

Elastic scattering allows macros and baryons to exchange momentum. The process has two undetermined parameters: the mass of the macro  $M$  and the interac-

tion cross section  $\sigma$ , generally taken to be the geometric cross-sectional area of the macro. Before proceeding, we pause to note that there remains a large range of the  $M$ – $\sigma$  parameter space which is still unprobed by experiment.

If a macro were to traverse through the Earth's atmosphere its energy deposition would excite the nitrogen molecules of air producing observable signals at fluorescence detectors. In this Letter we reexamine the methodology for estimating the sensitivity for macro detection at space-based and suborbital experiments. More concretely, we compare one approach for estimating the macro luminosity originally developed in the eighties [11] to a more recent examination of the problem [16]. We adopt three projects of the Joint Experiment Missions for Extreme Universe Space Observatory (JEM-EUSO) as reference in our discussion:

- the Mini-EUSO detector, currently taking data on board the International Space Station [17];
- the second generation Super-Pressure Balloon long duration flight (EUSO-SPB2), which has been approved by NASA to be launched in 2022 [18];
- the future Probe Of Extreme Multi-Messenger Astrophysics (POEMMA) mission [19].

Like meteoroids, macros are susceptible to rapid heat loss upon entering the Earth's atmosphere as a result of elastic collisions with the air molecules. Actually, it is at lower altitudes where the macro encounters the exponentially increasing atmospheric density and undergoes rapid heating along its path, which expands and radiates. The power dissipation rate of macros going through the atmosphere is given by

$$\frac{dE}{dt} \sim \rho_{\text{atm}} \sigma v^3, \quad (1)$$

where  $\rho_{\text{atm}}$  is the atmospheric density and  $v \sim 250$  km/s is the characteristic velocity of the Sun's galactic rotation [11]. To describe the atmospheric density variation we adopt an isothermal atmosphere,

$$\rho_{\text{atm}} = \rho_{\text{atm},0} \exp\left(-\frac{z}{z^*}\right), \quad (2)$$

where  $\rho_{\text{atm},0} = 10^{-3}$  g/cm<sup>3</sup> and  $z^* = 8$  km [20]. Now, the power dissipated to *useful* light is given by

$$L = \eta \rho_{\text{atm}} \sigma v^3, \quad (3)$$

where  $\eta$  is the luminous efficiency.

In the model of [11] it is assumed that the expanding hot cylinder emits black-body radiation, and its luminous efficiency is estimated to be

$$\eta_1 \sim 2 \times 10^{-5} \left(\frac{\bar{w}}{18}\right)^{3/2} \frac{\rho_{\text{water}}}{\rho_{\text{atm}}} \sim 0.04 \exp\left(\frac{z}{z^*}\right), \quad (4)$$

where  $\bar{w} \sim 29$  is the average molecular weight of air molecules and  $\rho_{\text{water}}$  is the water density. Substituting (4) into (3), the macro luminosity (for *model 1*) can be recast as

$$L_1 \approx 15 \left(\frac{M}{g}\right)^{2/3} x^{-2/3} \text{ W}, \quad (5)$$

or, as written in [11] assuming  $x = 1$ ,

$$L_1 \approx 1.5 \times 10^{-3} \left(\frac{M}{\mu g}\right)^{2/3} \text{ W}, \quad (6)$$

where

$$\sigma = 2.4 \times 10^{-10} \left(\frac{M}{g}\right)^{2/3} x^{-2/3} \text{ cm}^2, \quad (7)$$

with  $x \equiv \rho_m / \rho_s$ .

An alternative approach to describe the interactions of macros in the atmosphere, which includes a precise determination of the probability for transitions in a nitrogen plasma to produce a photon in the 350 to 400 nm detection range, has been recently developed in [16]. Within this model the luminous efficiency is given by

$$\eta_2 = 2 \times 10^5 \left(\frac{\sigma}{\text{cm}^2}\right)^2 \left(\frac{v}{250 \text{ km/s}}\right)^4 \left[\exp\left(-\frac{z}{10 \text{ km}}\right)\right]^4. \quad (8)$$

We note that the exponential comes from the height dependence of several functions on the atmospheric density, which are modelled as in (2), but with  $z^* = 10$  km. To remain consistent with the isothermal atmospheric model adopted for our calculations we write (8) as

$$\eta_2 \approx 1.15 \times 10^{-14} \left(\frac{M}{g}\right)^{4/3} x^{-4/3} \exp\left(-\frac{4z}{z^*}\right). \quad (9)$$

TABLE I: Macro luminosity parameters.

	<i>model 1</i>	<i>model 2</i>
$\alpha_i$	2/3	2
$\tilde{L}_i$ [W]	15	$4.32 \times 10^{-12}$
$f_i$	1	$\exp(-5z/z^*)$

With this in mind, the macro luminosity for *model 2* is given by

$$L_2 \approx 4.32 \times 10^{-12} \left(\frac{M}{g}\right)^2 x^{-2} \exp\left(-\frac{5z}{z^*}\right) \text{ W}. \quad (10)$$

By comparing (6) and (10) it is straightforward to see that *for a reference mass of 1 g,  $x = 1$ , and  $z = z^*$  there is a discrepancy of about 14 orders of magnitude between the predictions of the two models.*

The apparent magnitude of an object at a distance  $d$  and with luminosity  $L$  is defined as

$$\mathbf{m} = -\frac{5}{2} \log \frac{L}{4\pi d^2 \ell_0}, \quad (11)$$

where  $\ell_0 \approx 2.52 \times 10^{-8} \text{ W m}^{-2}$  [21]. For convenience, we rewrite (11) as

$$\mathbf{m} = 5 \log \frac{d}{d_*} - \frac{5}{2} \log \frac{L}{4\pi d_*^2 \ell_0}, \quad (12)$$

where  $d_*$  is any reference distance. The luminosity can be rewritten as

$$L_i = \tilde{L}_i \left(\frac{M}{g}\right)^{\alpha_i} x^{-\alpha_i} f_i(z), \quad (13)$$

with parameters given in Table I. Substituting (13) into (12) we obtain

$$\begin{aligned} \mathbf{m}_i &= -\frac{5}{2} \log \frac{\tilde{L}_i}{4\pi d_*^2 \ell_0} - \frac{5\alpha_i}{2} \log \left(\frac{M}{g} \frac{1}{x}\right) + 5 \log \frac{d}{d_*} \\ &\quad - \frac{5}{2} \log f_i(z). \end{aligned} \quad (14)$$

Following [11], we choose a scale  $d_* = 10$  km and a vertical observation altitude  $h \approx z + d$ , yielding

$$\mathbf{m}_1 = 0.811 - \frac{5}{3} \log \frac{M}{g} + 5 \log \frac{h-z}{10 \text{ km}} + \frac{5}{3} \log x, \quad (15a)$$

and

$$\begin{aligned} \mathbf{m}_2 &= 32.16 - 5 \log \frac{M}{g} + 5 \log \frac{h-z}{10 \text{ km}} + 5 \log x \\ &\quad + \frac{25}{2} \frac{z}{z^*} \frac{1}{\ln 10}. \end{aligned} \quad (15b)$$

For the purpose of comparison with [11], after setting  $x = 1$ , (15a) can be recast as

$$\mathbf{m}_1 = 10.811 - \frac{5}{3} \log \frac{M}{\mu g} + 5 \log \frac{d}{10 \text{ km}}. \quad (16)$$

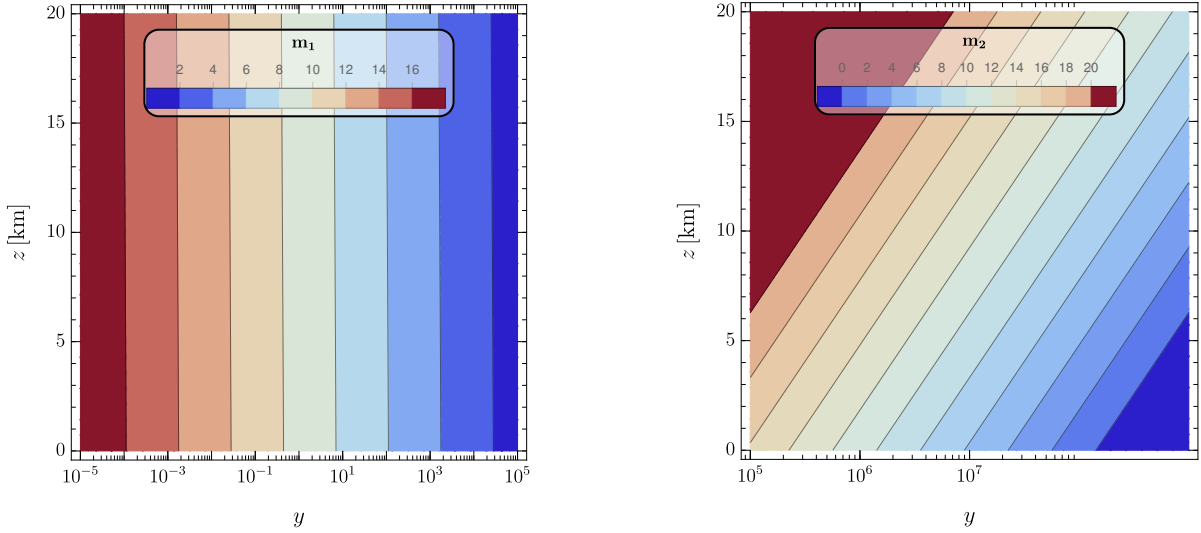


FIG. 1: Values of  $\mathbf{m}_1$  (left) and  $\mathbf{m}_2$  (right) as a function of  $y$  and  $z$  for POEMMA.

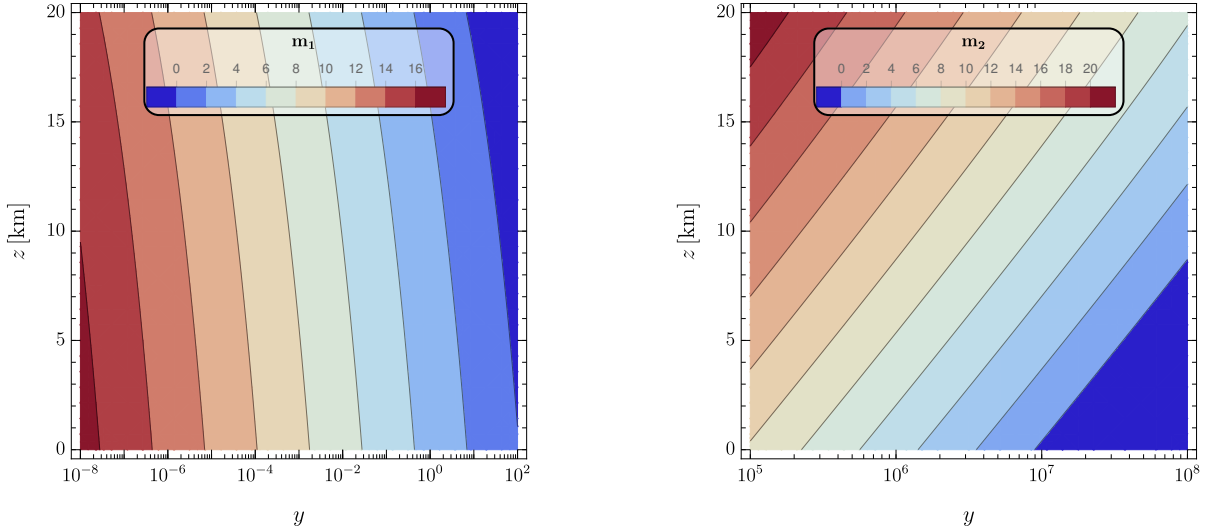


FIG. 2: Values of  $\mathbf{m}_1$  (left) and  $\mathbf{m}_2$  (right) as a function of  $y$  and  $z$  for EUSO-SPB2.

Setting  $h = 33$  km it is straightforward to see by comparing (15a) and (15b) that for our fiducial values ( $M = 1$  g,  $x = 1$ ,  $z = z^*$ ) the 14 orders of magnitude discrepancy in luminosity translate into a macro apparent magnitude difference  $\Delta \mathbf{m} = 36.8$ .

Mini-EUSO has demonstrated the capability to detect meteors [17]. Indeed Mini-EUSO (at an orbit of 400 km) is sensitive to meteors of apparent magnitude  $\mathbf{m} = 6$ , whereas POEMMA (at an orbit of 525 km) will be able to detect meteors of  $\mathbf{m} = 10$ . These estimates do not include effects due to potential atmospheric absorption, which will be discussed elsewhere. Macros travel much faster than meteors (which being bound to the solar system travel at less than 72 km/s relative to the Earth) allowing for clean discrimination among the atmospheric

signals. Moreover, clear differences in the meteor/macro light profiles have been observed in numerical simulations [22].

In order to study the observational sensitivity of JEM-EUSO instruments to  $M$  and  $x$  under both models we define the parameter  $y \equiv M/(x \text{ g})$ . In Fig. 1, we show constant apparent magnitude contours in the  $(y, z)$  plane, considering the observation altitude of POEMMA spacecraft. For comparison, in Fig. 2 we show same contours for EUSO-SPB2, which will fly at an altitude of about 33 km. There is no appreciable difference between the contours for Mini-EUSO and POEMMA, but of course they are sensitive to different apparent magnitudes. An apparent magnitude  $\mathbf{m} = 10$  corresponds to values  $y \approx 0.37$  for the first model, and  $y \approx 5 \times 10^5$  for the

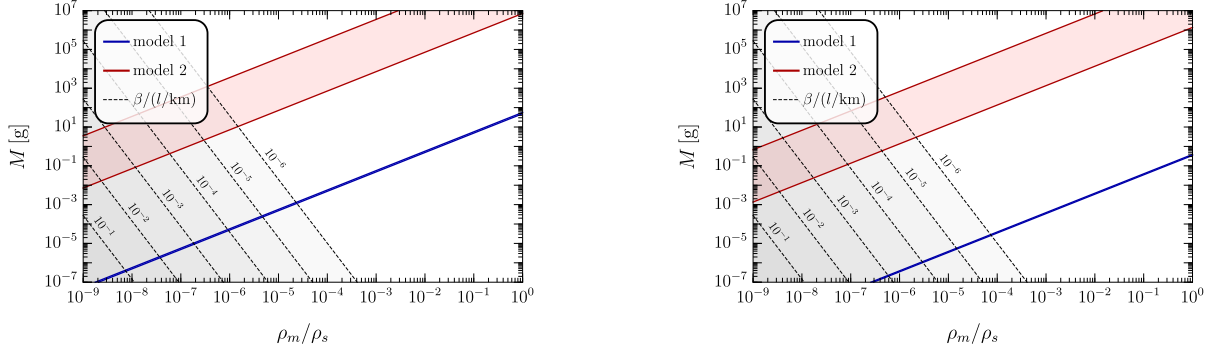


FIG. 3: Regions of the  $(x, M)$  parameter space for macros at altitudes from zero to 20 km which produce an apparent magnitude of  $m = 6$  (left) and  $m = 10$  (right). The regions below the lines produce larger magnitudes, so they are harder to observe than those above them. The dashed lines show the strength stability constraint  $\beta \ll 1$ .

second at  $z \approx z^*$ . Substituting this result into (15b) we can explore the sensitivity of Mini-EUSO and POEMMA scanning the  $(M, x)$  parameter space. The results of this exploration are encapsulated in Fig. 3 where we show the corresponding values in the  $(x, M)$  parameter space, for both models, in a generous range  $z \in [0 \text{ km}, 20 \text{ km}]$ .

The requirement of macro stability as it traverses the atmosphere sets an additional constraint on the cross section, as  $E_b M / m_b \gg \rho_{\text{atm}} \sigma v^2 l$ , where  $l$  is the length travelled by the macro through the atmosphere,  $m_b$  the baryon mass, and the macro binding energy is  $E_b \sim 10 \text{ eV} [\rho_m / (\text{g}/\text{cm}^3)]^{3/7}$  [24]. Substituting  $\sigma$  and  $\rho_{\text{atm}}$  from (2) and (7) this translates into a condition  $\beta \ll 1$ , where

$$\beta \equiv \frac{\rho_{\text{atm}} v^2 \sigma l}{E_b M / m_b} \approx 9 \times 10^{-13} \left( \frac{M}{\text{g}} \right)^{-1/3} x^{-23/21} \frac{l}{\text{km}}, \quad (17)$$

and where we have considered the upper bound on the density,  $\rho_{\text{atm}} = \rho_{\text{atm},0}$  to be conservative. The lines with constant  $\beta/l$ , which allow to determine the excluded areas for multiple lengths, are shown in Fig. 3. An upper bound for  $l$  may be set by assuming a trajectory tangent to the Earth's surface that starts and ends at a height  $z$  over the surface. In such case,  $(R_{\oplus} + z)^2 = R_{\oplus}^2 + (l/2)^2$ ,

which yields  $l \approx \sqrt{8R_{\oplus}z}$ , with a value of a few hundreds depending on the chosen  $z$ . A very conservative overestimate, for  $z \sim 20 \text{ km}$ , is  $l \sim 1000 \text{ km}$ .

All in all, we can conclude that:

- Mini-EUSO is sensitive to macros of  $x \sim 1.3 \times 10^{-8}$  for  $M \gtrsim 1 \text{ g}$ , and macros of  $x \sim 1$  for  $M \gtrsim 8.1 \times 10^7 \text{ g}$ ;
- the future POEMMA mission will be sensitive to macros of  $x \sim 6.1 \times 10^{-8}$  for  $M \gtrsim 1 \text{ g}$ , and macros of  $x \sim 1$  for  $M \gtrsim 1.6 \times 10^7 \text{ g}$ .

### Acknowledgments

This work has been partially supported by NASA Grants 80NSSC18K0464 (L.A.A., T.C.P., J.F.S.), 80NSSC18K0246 (J.E., A.V.O.), 80NSSC19K0626 (J.F.K.), 80NSSC18K0477 (F.S., L.W.), 17-APRA17-0066 (T.M.V.), and DoE Grant DE-SC-0010113 (M.H.R). M.E.B. is supported by Compagnia di San Paolo within the project 'ex-post-2018.' K.S. is supported by the National Science Centre in Poland, Grant 2020/37/B/ST9/01821. Any opinions, findings, and conclusions or recommendations expressed in this material are those of the authors and do not necessarily reflect the views of the NASA or DoE.

[1] J. L. Feng, *Dark matter candidates from Particle Physics and methods of detection*, Ann. Rev. Astron. Astrophys. **48**, 495-545 (2010) doi:10.1146/annurev-astro-082708-101659 [arXiv:1003.0904 [astro-ph.CO]].

[2] G. Steigman and M. S. Turner, *Cosmological constraints on the properties of weakly interacting massive particles*, Nucl. Phys. B **253**, 375 (1985). doi:10.1016/0550-3213(85)90537-1

[3] C. Dvorkin, K. Blum and M. Kamionkowski, *Constraining mark matter-baryon scattering with linear cosmology*, Phys. Rev. D **89**, no.2, 023519 (2014) doi:10.1103/PhysRevD.89.023519 [arXiv:1311.2937 [astro-ph.CO]].

[4] B. Penning, *The pursuit of dark matter at colliders—an overview*, J. Phys. G **45**, no.6, 063001 (2018) doi:10.1088/1361-6471/aabae7 [arXiv:1712.01391 [hep-ex]].

[5] S. Rappoccio, *The experimental status of direct searches for exotic physics beyond the standard model at the Large Hadron Collider*, Rev. Phys. **4**, 100027 (2019) doi:10.1016/j.revip.2018.100027 [arXiv:1810.10579 [hep-ex]].

[6] O. Buchmueller, C. Doglioni and L. T. Wang, *Search for dark matter at colliders*, Nature Phys. **13**, no.3, 217-223 (2017) doi:10.1038/nphys4054 [arXiv:1912.12739 [hep-ex]].

[7] T. Marrodán Undagoitia and L. Rauch, *Dark matter direct-detection experiments*, J. Phys. G **43**,

- no.1, 013001 (2016) doi:10.1088/0954-3899/43/1/013001 [arXiv:1509.08767 [physics.ins-det]].
- [8] J. M. Gaskins, **A review of indirect searches for particle dark matter**, *Contemp. Phys.* **57**, no.4, 496-525 (2016) doi:10.1080/00107514.2016.1175160 [arXiv:1604.00014 [astro-ph.HE]].
- [9] E. Witten, **Cosmic separation of phases**, *Phys. Rev. D* **30**, 272-285 (1984) doi:10.1103/PhysRevD.30.272
- [10] E. Farhi and R. L. Jaffe, **Strange matter**, *Phys. Rev. D* **30**, 2379 (1984) doi:10.1103/PhysRevD.30.2379
- [11] A. De Rujula and S. L. Glashow, **Nuclearites: A novel form of cosmic radiation**, *Nature* **312**, 734-737 (1984) doi:10.1038/312734a0
- [12] C. Alcock and A. Olinto, **Exotic phases of hadronic matter and their astrophysical application**, *Ann. Rev. Nucl. Part. Sci.* **38**, 161-184 (1988) doi:10.1146/annurev.ns.38.120188.001113
- [13] S. A. Chin and A. K. Kerman, **Possible longlived hyper-strange multi-quark droplets**, *Phys. Rev. Lett.* **43**, 1292 (1979) doi:10.1103/PhysRevLett.43.1292
- [14] Y. Bai, A. J. Long and S. Lu, **Dark quark nuggets**, *Phys. Rev. D* **99**, no.5, 055047 (2019) doi:10.1103/PhysRevD.99.055047 [arXiv:1810.04360 [hep-ph]].
- [15] D. M. Jacobs, G. D. Starkman and B. W. Lynn, **Macro dark matter**, *Mon. Not. Roy. Astron. Soc.* **450**, no.4, 3418-3430 (2015) doi:10.1093/mnras/stv774 [arXiv:1410.2236 [astro-ph.CO]].
- [16] J. Singh Sidhu, R. M. Abraham, C. Covault and G. Starkman, **Macro detection using fluorescence detectors**, *JCAP* **02**, 037 (2019) doi:10.1088/1475-7516/2019/02/037 [arXiv:1808.06978 [astro-ph.HE]].
- [17] S. Bacholle, *et al.*, **Mini-EUSO Mission to Study Earth UV Emissions on board the ISS**, *Astrophys. J. Suppl.* **253**, no.2, 36 (2021) doi:10.3847/1538-4365/abd93d [arXiv:2010.01937 [astro-ph.IM]].
- [18] L. Wiencke and A. Olinto [for the JEM-EUSO and POEMMA Collaborations], **The Extreme Universe Space Observatory on a super-pressure balloon II mission**, *PoS ICRC2019*, 466 (2020) doi:10.22323/1.358.0466 [arXiv:1909.12835 [astro-ph.IM]].
- [19] A. V. Olinto *et al.* [POEMMA Collaboration], **The POEMMA (Probe of Extreme Multi-Messenger Astrophysics) Observatory**, [arXiv:2012.07945 [astro-ph.IM]].
- [20] L. A. Anchordoqui, **Ultra-high-energy cosmic rays**, *Phys. Rept.* **801**, 1-93 (2019) doi:10.1016/j.physrep.2019.01.002 [arXiv:1807.09645 [astro-ph.HE]].
- [21] S. Weinberg, **Cosmology**, (Oxford University Press, 2008) ISBN:9780198526827
- [22] J. H. Adams *et al.* [JEM-EUSO Collaboration], **JEM-EUSO: Meteor and nuclearite observations**, *Exper. Astron.* **40**, no.1, 253-279 (2015) doi:10.1007/s10686-014-9375-4
- [23] T. C. Paul, S. T. Reese, L. A. Anchordoqui and A. V. Olinto, **EUSO-SPB2 sensitivity to macroscopic dark matter**, [arXiv:2104.01152 [hep-ph]].
- [24] J. S. Sidhu and G. Starkman, **Macroscopic dark matter constraints from bolide camera networks**, *Phys. Rev. D* **100**, no.12, 123008 (2019) doi:10.1103/PhysRevD.100.123008 [arXiv:1908.00557 [astro-ph.CO]].